Is [1-^{11}C]Putrescine Useful as a Brain Tumor Marker?

Emile M. Hiesiger, Joanna S. Fowler, Jean Logan, Jonathan D. Brodie, Robert R. MacGregor, David R. Christman, and Alfred P. Wolf

Departments of Neurosurgery and Psychiatry, New York University School of Medicine, New York, New York and Department of Chemistry, Brookhaven National Laboratory, Upton, New York

Our experience with ^{11}C-putrescine underscores the difficulty of finding a selective brain tumor tracer, uniquely incorporated by neoplastic glia or metastatic cells within brain, but not by the proliferating, nontransformed cells which constitute a normal pathophysiological reaction to various disease processes. Thirty-three patients with 36 lesions were studied with ^{11}C-putrescine to determine the specificity of labeled putrescine for tumor tissue. The uptake of ^{11}C-putrescine was correlated with local cerebral glucose metabolic rate in various lesions, including different types of tumors, to assess the relationship between ^{11}C-putrescine uptake and tumor biology. Carbon-11-putrescine uptake was similar in malignant tumor and benign, non-neoplastic lesions with blood-brain barrier breakdown, illustrating the lack of tumor specificity of this tracer. Carbon-11-putrescine was not well incorporated into poorly enhancing lesions, regardless of their pathology, emphasizing the requirement of a disrupted blood-brain barrier for ^{11}C-putrescine uptake. The ratio of ^{11}C concentration within lesions, compared to that in a region of interest in the contralateral brain, weakly correlated with an analogous ratio for local cerebral glucose metabolic rate in various lesions. Physiological processes not unique to tumors are associated with polyamine active transport and metabolism and contribute to the lack of tumor specificity of ^{11}C-putrescine. Carbon-11-putrescine appear to have less diagnostic utility than ^{18}FDG in brain tumors. The potential of ^{11}C-putrescine for evaluating the effect of antineoplastic therapy and providing prognostic information on brain tumors remains to be investigated.

J Nucl Med 1992; 33:192–199

Putrescine is a naturally occurring low molecular weight diamine. It is produced by the enzymatic decarboxylation of ornithine by ornithine decarboxylase (ODC) and serves as a precursor to the polyamines spermidine and spermine. We have previously reported the synthesis of ^{11}C-putrescine (^{11}C-PUT) and its examination as a tracer for polyamine metabolism in human cerebral malignancy using positron emission tomography (PET) (*1,2*). Labeled putrescine was chosen for several reasons including: (1) the known association of enhanced polyamine metabolism with stages of the cell cycle surrounding DNA synthesis, (2) the fact that ODC activity has been shown to correlate with the histopathological criteria of malignancy in both primary brain tumors and carcinomas, and (3) results from animal studies demonstrating high uptake of labeled putrescine in implanted gliomas (*3–11*). However, in spite of the strong link between putrescine metabolism and malignancy, a number of non-neoplastic processes are also associated with enhanced polyamine biosynthesis, possibly limiting the specificity of labeled putrescine as a tumor marker (*12–16*).

The initial evaluation of labeled putrescine as a tumor marker did not address tumor specificity (*2*). Accordingly, we are now reporting the results of ^{11}C-PUT studies on patients with various forms of central nervous system (CNS) pathology for the purpose of assessing the specificity of labeled putrescine in tumor tissue. In addition, the uptake of ^{11}C-PUT was correlated with local cerebral glucose metabolic rate (LCGMR) [measured by [1-^{11}C]2-deoxy-D-glucose (^{11}C-2DG) or 2-deoxy-2-[^{18}F]fluoro-D-glucose (^{18}FDG)] in different types of tumors for the purpose of assessing the relationship between ^{11}C-PUT uptake and tumor biology (*17,18*).

MATERIALS AND METHODS

Subjects

The present study includes 33 patients with 36 lesions in four major diagnostic categories (gliomas, necrosis, metastatic brain tumors, and miscellaneous). Data on seven patients from an earlier report were included in this analysis (*2*) (Tables 1 and 2). The sample includes the following lesions: 20 gliomas (16 of which are recurrent malignant gliomas), 4 cases of cerebral metastases (2 of which have multiple tumors), 4 cases of presumed treatment related necrosis (a non-neoplastic entity), and a miscellaneous group of non-neoplastic conditions (Table 1). A histological diagnosis was available on 17 patients, based on pathological specimens obtained within 2 ± 0.4 [mean ± standard error (s.e.m.)] wk (range 1–5 wk) of the PET study. In two other patients, the presumptive diagnosis of recurrent tumor (Case 9) or treatment related necrosis (Case 23) was confirmed by either biopsy or autopsy 9 or 12 mo following PET scanning, respectively. In 14 patients whose presumptive diagnoses were not

Received Mar. 18, 1991; revision accepted Sept. 9, 1991.

For reprints contact: Emile M. Hiesiger, MD, Dept. of Neurosurgery, New York University School of Medicine, 530 First Ave., New York, NY 10016.

confirmed pathologically, the diagnosis was based on clinical and radiological criteria (Table 1).

Radiological Studies

Patients routinely had CT scans, with and without contrast, within 1 mo prior to PET scanning (Table 1). Adequate contrast administration was confirmed on all scans by identifying enhanced cerebral vasculature. Contrast enhancement of lesions was subjectively rated by one author (EMH) as minimal (+), moderate (++), or marked (+++). One patient could not be given contrast due to renal insufficiency (Case 25B). Three patients with nonenhancing or poorly visualized lesions also underwent MRI scans less than 1 mo prior to PET scanning (Cases 2, 9, and 20).

PET Studies

Carbon-11-PUT, ^{11}C-2DG, and ^{18}FDG were prepared, PET studies were performed, and data were analyzed as described previously using PETT VI (spatial resolution at FWHM of 1.2 cm in the plane of section and 1.4 cm in the axial plane) (*1,2,19, 20*). Carbon-11-PUT uptake is reported as nCi/cc, corrected for a 10-mCi injected dose for lesion and control regions of interest (ROIs). The control ROI is a radiologically normal ROI, identical in size to that of the lesion, usually at the gray-white junction contralateral to the lesion (Table 2). The *rad-ratio* is the ratio of ^{11}C concentration in the lesion, compared to that in a contralateral ROI, after an injection of ^{11}C-putrescine.

Either an arterialized (23 cases) or arterial blood curve (5 cases) was measured for most subjects, as previously described (*2*), and an integral of plasma radioactivity, normalized for a 10-mCi injected dose, was obtained for all but five cases in which blood sampling was not successful (Cases 8, 16, 21, 22, and 33) (Table 2).

An ^{11}C-2DG scan (23 cases) or ^{18}FDG scan (Cases 3, 13, 14, 15, 17, 18, 20, 24) was performed 2 hr after the ^{11}C-PUT scan in 28 patients undergoing 31 PET scans. Mean plasma-glucose was 103 ± 5 mg/dl. Local cerebral glucose metabolic rates (LCGMR) (μmol/100 g/min) were determined for the same ROIs used to evaluate each putrescine study. The ratio of LCGMR in a lesion, compared to the that in a contralateral ROI, is referred to as the *met-ratio* and corresponds anatomically to the above described rad-ratio. Five patients had ^{11}C-PUT scans without evaluation of LCGMR (Cases 9, 16, 19, 29 and 30).

Data Analysis

Means ± s.e.m.s were calculated for ^{11}C-PUT uptake, LCGMR, and the respective lesion:control brain ratios for several diagnostic categories into which the lesions were grouped (Table 2). In the case of multifocal lesions, each lesion was evaluated as a separate data point. Three patients, with two lesions each, were scanned twice to evaluate either tumor recurrence (Case 23), treatment related necrosis (Case 25), or the effect of therapy on tumor and brain metabolism (Case 28) over time. In cases where more than one serial scan was obtained, only one was used for statistical analysis (Table 2).

RESULTS

Carbon-11-PUT Uptake

There was no significant difference between mean values for ^{11}C concentration in control ROIs between diagnostic categories. Overall, lesion ^{11}C concentration was 4.5-fold greater than that in control ROIs ($p < 0.001$, paired t-test). Mean tumor radioactivity and rad-ratio for all gliomas were not significantly different from the corresponding values obtained for either the malignant gliomas or the recurrent malignant gliomas. Therefore, gliomas were analyzed as a combined group. For 21 gliomas in 20 patients, mean tumor radioactivity was 362.4 ± 39.2 nCi/cc, 4.8-fold greater than the 75 ± 6.6 nCi/cc for control brain ($p < 0.001$, paired t-test). The corresponding rad-ratio for this group was 5.2 ± 0.6. Two of the three untreated malignant gliomas incorporated ^{11}C-PUT (Cases 1 and 3) with a rad-ratio greater than 2 (3.8 and 11.7, respectively). These values are similar to the rad-ratios for both primary and secondary treated, recurrent tumors.

For the six previously treated, recurrent metastatic tumors in four patients (Cases 25B, 26, 27, and 28A), the mean tumor radioactivity was 298.6 ± 48 nCi/cc, 5.7-fold greater than the 52.4 ± 8.9 nCi/cc for control brain ($p < 0.01$, paired t-test). The corresponding mean rad-ratio for this group was 6.5 ± 1.6, which was not significantly different from the corresponding values for patients with recurrent malignant gliomas (Table 2 and Figs. 1 and 2).

For the group of four patients with presumed treatment-related necrosis, the mean lesion radioactivity of 408.9 ± 158.3 nCi/cc was not significantly greater than that of control brain with a mean ROI radioactivity of 94.7 ± 18.3 nCi/cc. The rad-ratios for two patients in this group (Cases 23A and 24) were 5.4 and 3.0, respectively, within the range of the rad-ratios for malignant tumors (Table 2 and Figs. 1 and 2). However, the rad-ratio of three non-malignant lesions also fell well within the range of malignant tumors (Table 2 and Figs. 1 and 2). The case of a biopsy-proven demyelinating, inflammatory process had a rad-ratio of 3.9. In the biopsy-proven infarct, a rad-ratio of 3.9 was obtained. The meningioma, a tumor without a blood-tumor barrier (BTB), had a rad-ratio of 4.3.

The six lesions with a rad-ratio less than 2.0 all exhibited far less enhancement than the balance of the lesions with a higher rad-ratio (Tables 1 and 2). These six lesions included a nonenhancing malignant glioma (Case 2), the minimally-to-moderately enhancing untreated low-grade glioma (Case 4), a minimally enhancing presumably necrotic lesion (Case 21), a radiotherapeutically treated metastasis which no longer enhanced after treatment (Case 25A2), a partially thrombosed arteriovenous malformation (AVM) (Case 32) which demonstrated scant calcification and minimal enhancement, and a nonenhancing intraparenchymal cyst (Case 33).

For ^{11}C-PUT, the dose-corrected integral of plasma radioactivity was obtained for 31 lesions (Table 2). Plasma integrals were highly variable, ranging from 2925 nCi/cc × min to 11778 nCi/cc × min, with no correlation between plasma integral and lesion radioactivity. Therefore, only tissue uptake of radioactivity was examined.

LCGMR

Mean LCGMR and met-ratio for gliomas as a group were not significantly different from those of either malig-

TABLE 1
Patient Characteristics

Disease category	Case no.	Pathology*	CT enhancement	History: Pre-PET Surg.	Pre-PET RT	Pre-PET Chemo.	Post-PET Surg.
Glioma							
Untreated	1‡	R frontotemporal glioma III	+++	+§			+
	2	L frontal glioma II	−, (+ MRI)¶				+
	3	R trigone glioma III	+++				+
	4‡	L temporal glioma I**	++				+
Recurrent	5‡	R temporoparietal glioma II	+++	+	+	+	
	6‡	L temporal, frontal, and cerebellar malignant glioma	+++	+	+	+	+††
	7‡	L frontotemporal glioma III	+++	+	+	+	
	8	R occipital malignant glioma III	+++	+	+	+	+
	9	Pontomedullary primitive neuroectodermal tumor§§	(+ MRI)	+	+		+
	10	L thalamic glioma II	+++	+	+	+	+
	11	L frontal gliosarcoma	+++		+		+
	12	R temporal glioma III	+++	+	+	+	
	13	L occipital glioma III	+++	+	+	+	+
	14	R temporal glioma III	+++	+	+		+
	15	L temporal glioma III	+++	+	+	+	+
	16	L temporal glioma III	+++	+	+	+	+
	17	L frontal glioma III	+++	+	+	+	
	18	R frontal and callosal glioma III	+++	+	+		+
	19A1¶¶	L temporal glioma III	+++	+	+	+	
	19A2	L frontal glioma III part of multifocal tumor clinically	+++				
	20	L frontotemporal glioma III	+++	+	+	+	+
Necrosis: Subacute or chronic***	21‡	Bifrontal grade III glioma	+, (+ MRI)	+	+	+	
	22	R thalamic glioma II	+++	+	+		
	23A	IV ventricular glioma II/ependymoma and bilateral occipital necrosis	+++	+	+	+	
	23B†††	See above; recurrence vs. necrosis	+++				
	24‡‡‡	L parietal glioma III	+++	+	+	+	
Metastatic brain tumor§§§	25A1+2‡	NSCCL¶¶¶: cerebellar and occipital metastases	+++§§§§		+	+	
	25B1+2‡	NSCCL, cerebellar and occipital metastases: recurrence	N/A****				
	26	Breast carcinoma, midbrain metastasis	+++		+	+	
	27	Bladder carcinoma, R temporoparietal metastasis	+++		+		
	28A1+2	Melanoma, biparietal metastases	+++		+	+	
	28B1+2	Melanoma, biparietal metastases following iv chemotherapy	+++			+	
Miscellaneous	29	R temporal infarct	+++				+
	30	L occipital and R temporoparietal demyelinating, inflammatory process	+++				+††††
	31	L subfrontal meningioma, manic depressive psychosis	+++				
	32	R temporal partially thrombosed arteriovenous malformation	−				+
	33	R temporal intraparenchymal cyst	−				

* Glioma grading based on the Burger and Vogel classification (*40*).
† Surgery within 5 wk following PET unless otherwise noted.
‡ Used in previous publication (*2*).

nant gliomas or recurrent malignant gliomas (Table 2). Therefore, all gliomas were analyzed as a group. Mean LCGMR on seventeen tumors in seventeen patients was 39.9 ± 4.7 μmol/100 g/min, 1.5-fold greater than the contralateral brain regions which had a mean LCGMR of 26.2 ± 1.3 μmol/100 g/min ($p < 0.01$, paired t-test). The three untreated malignant gliomas had a mean LCGMR of 47.3 ± 1.4 μmol/100 g/min, which was not statistically greater than that of the recurrent tumors. The LCGMR values for tumor and contralateral brain reported here are consistent with literature values (*2,17*). However, the low-grade glioma (Case 4) had a LCGMR of 57.5 μmol/100 g/min and a met-ratio of 1.5, suggestive of a more malignant tumor.

The mean LCGMR for the six recurrent metastatic tumors was 25.6 ± 4.2 μmol/100 g/min, which was not significantly less than that of the recurrent gliomas or different from respective control brain. The four presumably necrotic lesions had a LCGMR of 24.8 ± 3.3 μmol/100 g/min and a mean met-ratio of 0.9 ± 0.2, not significantly less than the respective values for recurrent tumors. The LCGMR of the meningioma was hypermetabolic compared to the contralateral brain but both the AVM and cyst were hypometabolic with respect to a contralateral ROI.

For 17 gliomas for which both ^{11}C-PUT scans and LCGMR determinations were available, a weak, positive correlation existed between rad-ratio and met-ratio ($r = 0.56$. $p < 0.05$), but no correlation existed between lesion radioactivity and LCGMR. Likewise, for the 16 malignant gliomas within this group, there was a weak positive correlation between rad-ratio and met-ratio ($r = 0.55$, $p < 0.05$) but no correlation between tumor radioactivity and LCGMR. For 12 recurrent gliomas, there was no correlation between tumor radioactivity and LCGMR nor between tumor rad-ratio and met-ratio. There was a weak positive correlation between rad-ratio and met-ratio for the combined sample of twenty four gliomas, metastases, and the meningioma ($r = 0.45$, $p < 0.05$), but no correlation between tumor radioactivity and LCGMR. Overall, there were weak positive correlations between rad-ratio and met-ratio ($r = 0.50$, $p < 0.01$) and between lesion radioactivity and LCGMR ($r = 0.38$, $p < 0.01$) for 31 lesions in which both ^{11}C-PUT uptake and LCGMR were evaluated.

Serial Studies

Three patients were scanned twice: one with treatment-related necrosis (Case 23), one with recurrent metastases (Case 25), and one patient with bilateral metastatic brain tumors scanned before and after chemotherapy (Case 28). Small changes in both lesion and contralateral radioactivity over a 10-mo interval were observed in the case of bioccipital treatment related necrosis (Case 23). These changes resulted in only a 13% decrease in the lesion rad-ratio. There was no similar change in LCGMR for the lesion or contralateral ROI over the same interval.

For the recurrent metastatic tumors (Case 25B), there was a three-fold increase in tumor radioactivity and a two-fold increase in rad-ratio compared to baseline values obtained 4 mo previously (Case 25A) (*2*). Similarly, one of these recurrent metastases (Case 25B1) demonstrated a three-fold increase in LCGMR and two-fold increase in met-ratio compared to baseline values, whereas the other recurrent tumor (25B2) exhibited no change in LCGMR over the same time period.

The last patient who underwent serial scans (Case 28) was scanned at baseline 12 wk after cranial irradiation for metastatic melanoma and prior to chemotherapy. Chemotherapy was administered following the initial PET scan and the patient was rescanned 3 wk after chemotherapy. Comparison between the first and second PET series revealed that the post-treatment rad-ratios for both tumors decreased only negligibly compared to the pretreatment ratio. However, the LCGMR after treatment *increased* in control brain more than in the tumors so that the post-treatment met-ratios *decreased* by 25% and 9%, respectively, compared to the pre-treatment ratios. In this case, the patient's clinical status and the CT appearance of the intracranial tumors did not change between the two PET studies.

[§] Biopsy.

[¶] MRI scans were all T1/T2 studies without gadolinium; a positive (+) MRI represents an increased signal on a T2-weighted image.

[**] No recurrence in 24 mo.

[††] Autopsy 1 mo after PET: multifocal glioma III.

[§§] No CT scan; surgery 9 mo after PET. This tumor is a malignant primary brain tumor, but not a glioma.

[¶¶] Code to numbering system of cases in Table 1 and Table 2: the first integer identifies the patient, the following letter denotes the number of scans where more than one scan was performed (A = 1 scan, B = 2 scans), and the final integer refers to a given lesion where multiple lesions exist within the same brain (lesion 1, 2, etc).

[***] Interval between original diagnosis and PET: Case 21 (38 mo), Case 22 (10 yr), Case 23A (6 yr), Case 23B (7 yr), Case 24 (8 mo).

[†††] Autopsy 12 mo after PET: radiation necrosis, no tumor.

[‡‡‡] No recurrence in 3.5 yr.

[§§§] Interval between PET scans: Case 25 (4 mo) and Case 28 (3 wk).

[¶¶¶] NSCCL = Non-small-cell carcinoma of the lung.

[****] Noncontrast scan only.

[††††] Left occipital biopsy.

[§§§§] Case 25A1 enhanced (cerebellar tumor), but Case 25A2 did not enhance (occipital tumor).

TABLE 2
Means and SEMs for ^{11}C-PUT Uptake and LCGMR

Diagnostic category	Case no.	^{11}C-Putrescine				LCGMR		
		Lesion nCi/cc*	Control nCi/cc*	Rad ratio†	Plasma integral nCi/cc × min*	μmol/100 g/min Lesion	μmol/100 g/min Control	Met ratio‡
Glioma								
Untreated, malignant	1	229.8	59.8	3.8	3771.8	48.9	24.8	2.0
	2	119.9	67.1	1.8	4000.0§	10.0	27.0	0.4
	3	675.7	58.1	11.6	6995.9	83.0	27.0	3.1¶
Untreated, low-grade	4	65.6	43.7	1.5	2925.3	57.5	39.7	1.4
Recurrent malignant	5	254.2	91.8	2.8	4295.3	52.9	29.5	1.8
	6	300.6	78.7	3.8	4719.4	35.2	26.4	1.3
	7	428.0	136.2	3.1	4043.7	51.9	27.1	1.9
	8	492.7	145.5	3.4	N/A	21.1	24.0	0.9
	9	370.8	108.8	3.4	5133.5	N/A	N/A	N/A
	10	216.3	79.2	2.7	6715.7	24.0	28.8	0.8
	11	187.1	73.1	2.6	9033.8	47.7	22.4	2.1
	12	339.3	49.2	6.9	6160.7	22.8	17.5	1.3
	13	275.5	52.6	5.2	4582.0	36.7	27.4	1.3¶
	14	565.3	106.2	5.3	6083.2	69.1	29.6	2.3¶
	15	629.4	97.9	6.4	7707.7§	36.3	28.2	1.3¶
	16	541.1	69.3	7.8	N/A	N/A	N/A	N/A
	17	364.4	55.4	6.6	11778.4§	18.1	24.0	0.8¶
	18	344.2	69.4	5.0	5604.1§	28.0	28.1	1.0¶
	19A1	291.3	36.6	8.0	4383.5	N/A	N/A	N/A
	19A2	219.5	36.6	6.0	4383.5§	N/A	N/A	N/A
	20	700.2	60.7	11.5	5528.6	35.3	14.0	2.5¶
Gliomas	mean	362.4	75.0	5.2	5747.9	39.9	26.2	1.5
	s.e.m.	39.2	6.5	0.6	497.6	4.7	1.3	0.2
	n	21	21	21	18	17	17	17
Malignant gliomas	mean	377.3	76.6	5.4	5914.0	38.8	25.4	1.6
	s.e.m.	38.1	6.7	0.6	507.3	4.8	1.1	0.2
	n	20	20	20	17	16	16	16
Recurrent gliomas	mean	383.5	79.2	5.3	6126.4	36.9	25.2	1.5
	s.e.m.	37.1	7.7	0.6	574.0	4.2	1.3	0.2
	n	17	17	17	14	13	13	13
Necrosis: Subacute or chronic	21	187.7	144.6	1.3	N/A	33.7	34.8	1.0
	22	854.4	97.5	8.8	N/A	23.6	21.0	1.1
	23A	415.4	76.9	5.4	4747.9	24.0	20.0	1.2
	23B**	383.4	81.8	4.7	9565.7	23.8	19.5	1.2
	24	177.9	59.8	3.0	8449.4	17.8	39.5	0.5¶
	mean	408.8	94.7	4.6	6598.7	24.8	28.8	0.9
	s.e.m.	158.3	18.3	1.6	1850.7	3.3	4.9	0.2
	n	4	4	4	2	4	4	4
Metastatic brain tumor	25A1**	148.1	41.0	3.6	3564.7	15.2	24.2	0.6
	25A2**	69.3	37.8	1.8	3564.7	17.1	25.2	0.7
	25B1	426.8	66.4	6.4	3884.1	43.8	35.4	1.2
	25B2	232.5	52.9	4.4	3884.1	16.7	30.6	0.5
	26	306.7	88.0	3.5	3917.5	25.0	25.0	1.0
	27	103.3	38.3	2.7	5044.6	14.4	16.6	0.9
	28A1	394.9	29.0	13.6	3834.5	27.5	16.9	1.6
	28A2	327.3	39.9	8.2	3834.5	26.2	23.4	1.1
	28B1**	405.3	31.6	12.8	6180.6	32.0	27.8	1.2
	28B2**	315.7	40.4	7.8	6180.6	28.0	28.0	1.0
	mean	298.6	52.4	6.5	4066.6	25.6	24.7	1.1
	s.e.m.	48.0	8.9	1.6	196.1	4.2	3.0	0.1
	n	6	6	6	6	6	6	6
Miscellaneous								
Infarct	29	285.3	73.9	3.9	4110.2	N/A	N/A	N/A
Inflammatory process	30	275.9	70.5	3.9	6238.4	N/A	N/A	N/A
Meningioma	31	383.3	89.6	4.3	5363.2	23.5	18.9	1.2
AVM	32	80.7	66.5	1.2	5616.8	20.1	31.3	0.6
Cyst	33	57.9	105.3	0.6	N/A	17.6	25.6	0.7

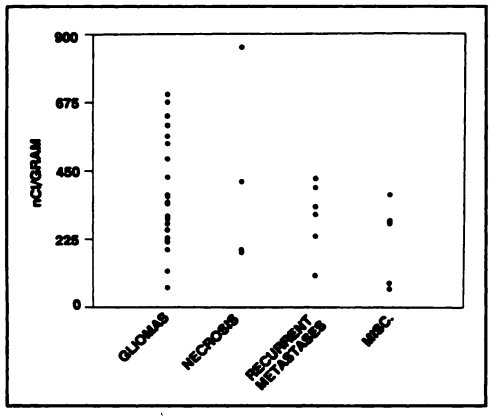

FIGURE 1. The range of ^{11}C concentration (nCi/cc lesion) within lesions is compared across four different diagnostic categories. The lesion radioactivity values in this table are taken from the data in Table 2 and are corrected for a 10-mCi injected dose.

DISCUSSION

Earlier PET studies on ^{11}C-PUT uptake into tumors demonstrate that the radioligand is incorporated into tumors with blood-tumor breakdown within minutes of injection, remaining there for the duration of a 45-min PET scan (*2*). This, and data on the active transport system in brain for putrescine, suggest that putrescine taken up into various brain lesions is trapped intracellularly (*21*). However, if ^{11}C-PUT is to be more than a marker of blood-brain barrier (BBB) and BTB integrity, its uptake must be linked to lesion cellular polyamine metabolic requirements. PET measurement of lesion polyamine metabolism using ^{11}C-PUT is predicated on a predictable, stable relationship between lesion uptake of ^{11}C-PUT, ODC activity, and polyamine metabolism. In the case of tumors, ^{11}C-PUT uptake should reflect aggregate tumor polyamine metabolic demands, proliferative activity, and biological aggressiveness (*3–11,22,23*).

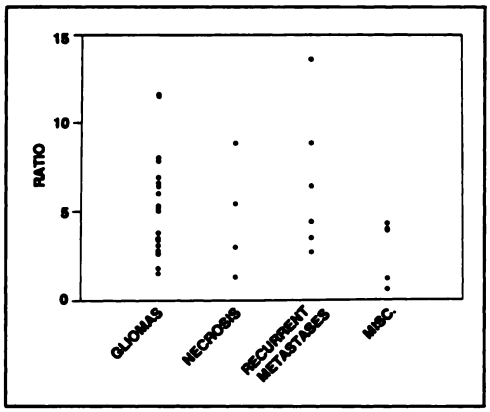

FIGURE 2. The range of rad-ratios (^{11}C concentration (nCi/cc) in lesion: contralateral brain) within lesions is compared across four different diagnostic categories. The ratios in this table are taken from the rad-ratios in Table 2 and are based on data corrected for a 10-mCi injected dose.

In in vivo tumor models, it has been demonstrated that tumor cells are able to incorporate and metabolize exogenous putrescine in proportion to intracellular polyamine metabolic requirements and availability of endogenous putrescine (*11,24*). However, both an in vitro evaluation of human brain tumors and an in vivo study of experimental brain tumors have shown that polyamine conversion of incorporated exogenous putrescine ranged from 4% to 11%, which did not correlate with the amount of putrescine incorporation (*25,26*). These latter experiments suggested that aggregate tumor polyamine conversion of incorporated putrescine reflects DNA synthesis in the viable, dividing cells (*22*). Unfortunately, the above in vivo animal tumor models generated conflicting data on the relationship between putrescine uptake and conversion. In vivo human studies may be required to clarify the relationship between putrescine uptake and polyamine metabolism in human brain tumors.

The present comparative PET study of four different disease categories illustrates the lack of tumor specificity of ^{11}C-PUT but suggests a potential for this probe in monitoring brain tumor therapy and determining prognosis. A number of different CNS pathological entities were studied. These included both neoplastic and nonneoplastic processes of BBB breakdown (such as necrosis, infarct or a demyelinating, inflammatory process). A meningioma (a histologically benign tumor devoid of a BTB) and several poorly or nonenhancing lesions were also studied.

These studies indicate that ^{11}C-PUT uptake is (1) not specific for malignant tumors and (2) can reflect a number of factors other than mitotic index or tumor biology. More specifically, the diagnostic accuracy of PET studies using ^{11}C-PUT in brain is limited by nonspecific factors common to CNS lesions. Distinct CNS disease entities share similar pathophysiological and histopathological characteristics which may result in ^{11}C-PUT uptake. For example, both

* Normalized for a 10-mCi injected dose. The values in the lesion and control columns are graphically depicted in Figures 1 and 2. The data from Cases 1, 4, 5, 6, 7, 21, and 25 were used in a previous publication, as noted in Table 1 (*2*). In that publication, blood-to-tissue influx constants (K_i) were used to describe the uptake of ^{11}C-putrescine. An explanation of our decision not to continue using these constants in this report is given in the Appendix.

† Rad-ratio is the ratio of ^{11}C concentration in a lesion, compared to that in a contralateral ROI, after an injection of ^{11}C-putrescine.

‡ The ratio of LCGMR in a lesion, compared to that in a contralateral ROI, is referred to as the met-ratio and corresponds anatomically to the above described rad-ratio. Plasma integrals are based on arterialized blood samples except where noted by §, indicating arterial sampling. LCGMR determinations were made using ^{11}CDG except where noted by ¶, indicating an ^{18}FDG study. N/A = not available or applicable.

** Excluded from statistical analyses except when evaluating changes between serial scans. Values in Cases 23A and 23B were nearly identical. Cases 25A1 and 25A2 were not an active recurrence. Cases 28B1 and 28B2 were scanned after therapy for recurrent disease.

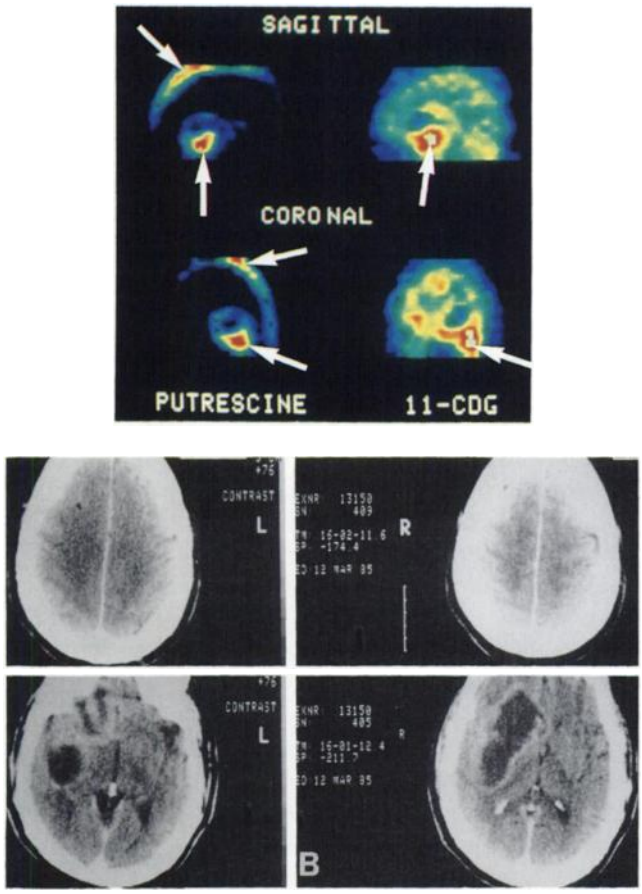

FIGURE 3. (A) PET scans with ^{11}C-putrescine and ^{11}C-2DG on a patient (Case 1, Tables 1 and 2) with a deep right frontotemporal cystic malignant glioma, scanned 48 hr after placement of a burr hole and an unsuccessful attempt at needle aspiration of the cystic lesion. Note the significant ^{11}C-putrescine uptake in the tumor and over the ipsilateral convexity, especially around the small scalp incision, burr hole and site of dural, meningeal, and brain puncture with the biopsy needle (arrows). The ^{11}C-2DG scan demonstrates a hypermetabolic tumor with respect to surrounding or contralateral brain and relative hypometabolism in the area of brain extending from tumor peripherally to the cortex (arrows). Clinical examinations and CT scans (B) obtained the day of the needle biopsy and 4 days following the PET studies failed to demonstrate any epidural or subdural fluid collection, or evidence of dural, meningeal or cortical involvement with tumor.

the nonspecific BBB breakdown characteristic of various contrast-enhancing CNS lesions and the platelet aggregation seen in various hemorrhagic lesions (tumors, infarcts) may influence ^{11}C-PUT uptake (*2,12,14,27*). To the extent that uptake of ^{11}C-PUT is linked to lesion polyamine metabolism, nonspecific influences on polyamine metabolism may also affect ^{11}C-PUT uptake. For example, polyamine metabolism is linked to the synthesis of RNA as well as that of DNA (*28*). Increased ODC activity and putrescine synthesis also has been demonstrated in CNS endothelial cells responding to a stimulus producing vasogenic edema and BBB breakdown, and in postischemic brain cells (*12–16*). Thus, both dividing cells (neoplastic cells, proliferating endothelia, reactive glia, macrophages, and fibroblasts) and nondividing cells (inflammatory cells and platelets) in tumors, infarcts, demyelinating lesions, vasculitis, and arteriovenous malformations, for example, may actively incorporate and metabolize putrescine. For example, in Figure 3A, the enhanced ^{11}C-putrescine uptake over the convexity presumably is a result of local, microscopic, post-surgical hemorrhage and platelet aggregation within the superficial tissues.

Nevertheless, the above PET data suggest that ^{11}C-PUT may have a role in evaluating therapy and in providing prognostic information on tumors. The preliminary studies on patients before and after tumor recurrence or during initiation of chemotherapy suggested that both tumor LCGMR and ^{11}C-PUT uptake may be useful for evaluating therapeutic efficacy. Other PET studies have demonstrated a 40% reduction in tumor LCGMR after radiation and chemotherapy of malignant gliomas (*29*). In vivo and in vitro studies have demonstrated a 25%–60% reduction in endogenous polyamine concentrations following radiation and chemotherapy (*30–32*). Anti-neoplastic therapy has also been shown to inhibit multiple enzymatic steps in the polyamine biosynthetic pathway (*30–32*). To the extent ^{11}C-PUT uptake is linked to intracellular polyamine biosynthetic demands, anti-neoplastic therapy may result in reduced incorporation of exogenous putrescine. Such therapy also may deleteriously affect the active transport system responsible for putrescine cellular uptake. Radiotherapy may also result in small vessel thrombosis, impeding putrescine entry into tumors (*33–35*). Therefore, tumors responding satisfactorily to treatment should exhibit diminished tumor uptake of ^{11}C-PUT, compared to uptake values obtained prior to treatment or at recurrence.

The correlations between rad-ratio and met-ratio suggest that ^{11}C-PUT uptake may have prognostic importance. Two observations support this conclusion. First, those lesions with a significantly disrupted BBB (and possibly with the greatest polyamine metabolic requirements) were also the most hypermetabolic lesions and presumably the most biologically aggressive neoplasms (*17,18*). In support of this observation, the degree of enhancement on CT scans, a measure of BBB disruption, has been correlated with histological grade and inversely related to survival (*36,37*). Second, tumor LCGMR has diagnostic significance, superior to CT in some cases, as well as prognostic importance (*17,18,38–39*). Since ^{11}C-PUT uptake is correlated with LCGMR, ^{11}C-PUT uptake may have prognostic significance as well, regardless of the precise factors responsible for its incorporation into tumors.

CONCLUSION

The data in this report suggest that ^{11}C-PUT uptake is similar in malignant tumors and benign or non-neoplastic lesions with BBB breakdown. In each case, exogenous putrescine may be incorporated (and possibly metabolized) by a different mixture of cells. The ability of ^{11}C-PUT to diagnose tumors or reflect tumor polyamine me-

tabolism, mitotic activity, and biological behavior is limited by at least four factors. First, ^{11}C-PUT is incorporated into both neoplastic and non-neoplastic brain lesions with a disrupted BBB and may be actively incorporated into both malignant and non-neoplastic cells. Second, the exact relationship between the active transport of putrescine into cells and cellular polyamine requirements is unknown. Third, to the extent that ^{11}C-PUT uptake may be related to aggregate cellular polyamine metabolism within lesions, cellular polyamine metabolism is linked to RNA and not just DNA synthesis (*28*). Finally, ^{11}C-PUT does not cross the intact BBB or BTB, which limits its utility as an imaging ligand to enhancing lesions or the enhancing portion of lesions (*27*).

Therefore, ^{11}C-PUT appears to have more limited *diagnostic* utility than ^{18}FDG or ^{11}C-2DG. Like ^{18}FDG, ^{11}C-PUT may have a role in *evaluating* the effect of antineoplastic *therapy* on tumor biochemistry and physiology (*29*). It is not yet known whether ^{11}C-PUT, like ^{18}FDG, may be useful for *prognosis* within a given class of tumor (*18*). Our experience with ^{11}C-PUT underscores the difficulty of finding a selective brain tumor tracer, uniquely incorporated by neoplastic glia or metastatic cells within brain, but not by the proliferating, nontransformed cells which constitute a normal pathophysiological reaction to various disease processes.

APPENDIX

Brain influx constants (K_i) (expressed in $ml_{(plasma)}$ $cc_{(tissue)}^{-1} min^{-1}$) were not used in this publication because of difficulties in obtaining individual patients' plasma metabolites, needed to correctly calculate K_is. Even in our prior publication on ^{11}C-putrescine, it was stated that the K_i data on all eight patients was based on metabolite data from one patient (*2*). Extrapolation of the metabolite data from one patient to others for purposes of determining the K_is may yield erroneous results. Therefore, we decided not to pursue the use of K_is in this larger series.

Data from seven of the original eight patients from the previous publication were used in this series (Tables 1 and 2) (*2*). The K_is for tumor, control brain, and the tumor:contralateral K_i ratio for the seven cases derived from the previous publication are as follows: Case 1: 0.81, 0.21, 3.86; Case 4: 0.033, 0.021, 1.57; Case 5: 0.084, 0.029, 2.89; Case 6: 0.084, 0.020, 4.20; Case 7: 0.143, 0.043, 3.32; Case 21: no K_is were available; Case 25A1: 0.057, 0.025, 2.28; Case 25A2: 0.033, 0.018, 1.83; Case 25B1: 0.155, 0.024, 6.45; and Case 25B2: 0.085, 0.024, 3.54.

ACKNOWLEDGMENTS

This research was carried out at Brookhaven National Laboratory and New York University School of Medicine. Supported in part by the U.S. Department of Energy, the Office of Health and Environmental Research, and NIH grant NS 15638. The authors wish to thank the patients and their families for cooperating in this study, Ajax George, MD for neuroradiological consultation, and Arlene Wise for patient data management. The authors are also grateful to Karin Karlstrom, Elizabeth Jellett, and Colleen Shea for radiopharmaceutical synthesis; Payton King for plasma assays; David Schlyer, Donald Warner, Robert Carciello and Babe Barrett for cyclotron operations; and Theodore Johnson and Noelwah Netusil for patient care.

REFERENCES

1. McPherson DW, Wolf AP, Fowler JS, Arnett CD, Brodie JD, Volkow N. Synthesis and biodistribution of no-carrier-added [1-^{11}C]putrescine. *J Nucl Med* 1985;26:1186–1189.
2. Hiesiger E, Fowler JS, Wolf AP et al. Serial PET studies of human cerebral malignancy with [1-^{11}C]putrescine and [1-^{11}C]2-deoxy-D-glucose. *J Nucl Med* 1987;28:1251–1261.
3. Friedman SJ, Bellantone RA, Canellakis ES. Orithine decarboxylase activity in synchronously growing Don C cells. *Biochem Biophys Acta* 1972;261:188–193.
4. Russell DH, Stambrook PJ. Cell cycle specific fluctuations in adenosine 3′:5′-cyclic monophosphate and polyamines of Chinese hamster cells. *Proc Natl Acad Sci* 1975;72:1482–1486.
5. Heby O, Sarna GP, Marton LJ, Omine M, Perry S, Russell DH. Polyamine content of AKR leukemic cells in relation to the cell cycle. *Cancer Res* 1973;33:2959–2964.
6. Heby O, Marton LJ, Zardi L, Russell DH, Baserga R. Changes in polyamine metabolism in WI-38 cells stimulated to proliferate. *Exp Cell Res* 1975;90:8–14.
7. Heby O, Andersson G. Polyamines and the cell cycle. In: Gaugas JM, ed. *Polyamines in biomedical research.* New York: Wiley; 1980:17–34.
8. McCann PP, Tardif C, Mamont PS, Schuber F. Biphasic induction of ornithine decarboxylase and putrescine levels in growing HTC cells. *Biochem Biophys Res Comm* 1975;64:336–341.
9. Scalabrino G, Ferioli ME. Degree of enhancement of polyamine biosynthetic decarboxylase activities in human tumors: a useful new index of degree of malignancy. *Cancer Detection Prevention* 1985;8:11–16.
10. Glikman P, Vegh I, Pollina MA, Mosto AH, Levy CM. Ornithine decarboxylase activity, prolactin in blood levels, and estradiol and progesterone receptors in human breast cancer. *Cancer* 1987;60:2237–2243.
11. Volkow N, Goldman SS, Flamm ES, Cravioto H, Wolf AP, Brodie JD. Labeled putrescine as a probe in brain tumors. *Science* 1983;221:673–675.
12. Koenig H, Goldstone AD, Chung YL. Blood-brain barrier breakdown in brain edema following cold injury is mediated by microvascular polyamines. *Biochem Biophys Res Comm* 1983;116:1039–1048.
13. Trout JJ, Koenig H, Goldstone AD, Chung YL. Blood-brain barrier breakdown by cold injury. *Lab Invest* 1986;55:622–631.
14. Nadler SG, Takahashi MT. Putrescine transport in human platelets. *Biochem Biophys Acta* 1985;812:345–352.
15. Dempsey RJ, Maley B, Olson J, Cowen DE, Maley M, Roy MW. Ornithine decarboxylase activity and immunohistochemical location in post-ischemic brain. *J Cereb Blood Flow Metab.* 1987;7(suppl 1):S73.
16. Paschen W, Schmidt-Kastner R, Djuricic B, Meese C, Linn F, Hossman K-A. Polyamine changes in reversible cerebral ischemia. *J Neurochem* 1987;49:35–37.
17. Di Chiro G. Positron emission tomography using [^{18}F]fluorodeoxyglucose in brain tumors: a powerful diagnostic and prognostic tool. *Invest Radiol* 1986;22:360–371.
18. Patronas NJ, Di Chiro G, Kufta C, et al. Prediction of survival in glioma patients by means of positron emission tomography. *J Neurosurg* 1985;62:816–822.
19. MacGregor RR, Fowler JS, Wolf AP, Shiue C-Y, Lade RE, Wan CN. A synthesis of ^{11}C-2-deoxy-D-glucose for regional metabolic studies. *J Nucl Med* 1981;22:800–803.
20. Hamacher K, Coenen HH, Stocklin G. Efficient stereospecific synthesis of no-carrier-added 2-[^{18}F]-fluoro-2-deoxy-D-glucose using aminopolyether supported nucleophilic substitution. *J Nucl Med* 1986;27:235–238.
21. Smith LL, Wyatt I. The accumulation of putrescine into slices of rat lung and brain and its relationship to the accumulation of paraquat. *Biochem Pharm* 1981;30:1053–1058.
22. Hoshino T, Barker M, Wilson CB. Cell kinetics of human gliomas. *J Neurosurg* 1972;37:15–26.
23. Hoshino T, Nagashima T, Kyung GC, et al. Variability in the proliferative potential of human gliomas. *J Neuro Oncol* 1989;7:137–143.
24. Chaney JE, Kobayashi K, Goto R, Digenis GA. Tumor selective enhancement of radioactivity uptake in mice treated with alpha-difluoromethylornithine prior to administration of ^{14}C-putrescine. *Life Sci* 1983;32:1237–1241.
25. Goldman SS, Volkow ND, Brodie J, Flamm ES. Putrescine metabolism in human brain tumors. *J Neuro Oncol* 1986;4:23–29.
26. Warnick RE, Pietronegro DD, McBride DQ, Flamm ES. In vivo metabo-

lism of radiolabeled putrescine in gliomas. Implications for positron emission tomography of brain tumors. *Neurosurg* 1988;23:464–469.
27. Shin WW, Fong WF, Pang SF, Wong P C-L. Limited blood-brain barrier transport of polyamines. *J Neurochem* 1985;44:1056–1059.
28. Tabor CW, Tabor H. 1,4-Diaminobutane (putrescine), spermidine, and spermine. *Ann Rev Biochem* 1976;915:285–306.
29. Ogawa T, Uemura K, Shishido F, et al. Changes of cerebral blood flow, and oxygen and glucose metabolism following radiochemotherapy of gliomas: a PET study. *J Comp Assist Tomog* 1988;12:290–297.
30. Russell DH, Durie BGM. *Polyamines as biochemical markers of malignancy.* New York: Raven Press; 1978:15–41.
31. Cavanaugh PF, Zlatko PP, Porter CW. Enhancement of 1,3-bis [2-chloroethyl]-1-nitrosourea-induced cytotoxicity and DNA damage by alpha-difluoromethylornithine in L1210 leukemia cells. *Cancer Res* 1984;44:3856–3861.
32. Pegg AE, McCann PP. Polyamine metabolism and function. *Am J Physiol* 1982;243:C212–C221.
33. Hopewell JW. Late radiation damage to the central nervous system: a radiobiological interpretation. *Neuropath Applied Neurobiol* 1979;5:329–349.
34. Conomy JP, Kellermeyer RW. Delayed cerebrovascular consequences of therapeutic radiation. *Cancer* 1975;36:1702–1708.
35. De Ruiter J, Van Putten LM. Measurement of blood flow in the mouse tail after irradiation. *Radiation Res* 1975;61:427–438.
36. Butler AR, Horii SC, Kricheff II, Shannon MB, Budzilovich GN. Computed tomography in astrocytomas. A statistical analysis of the parameters of malignancy and the positive contrast-enhanced CT scan. *Radiology* 1978;129:433–439.
37. Andreou J, George AE, Wise A, et al. Prognostic criteria of survival after malignant glioma surgery. *AJNR* 1983;4:488–490.
38. Di Chiro G, Oldfield E, Wright DC, et al. Cerebral necrosis after radiotherapy and/or intraarterial chemotherapy for brain tumors: PET and neuropathologic studies. *AJNR* 1988;150:189–197.
39. Valk PE, Budinger TF, Levin VA, Silver P, Gutin PH, Doyle WK. PET of malignant cerebral tumors after interstitial brachytherapy. Demonstration of metabolic activity and correlation with clinical outcome. *J Neurosurg* 1988;69:830–838.
40. Burger PC, Vogel FS, Green SB, Strike TA. Glioblastoma multiforme and anaplastic astrocytoma: pathologic criteria and prognostic implications. *Cancer* 1985;56:1106–1111.

EDITORIAL

Carbon-11-Putrescine: Back to the Drawing Board

The oft-stated aim of PET neuro-oncologists is to exploit metabolic differences between tumor tissue and surrounding normal brain in order to improve tumor localization and permit non-invasive determinations of tumor histology and growth rate that can be used to assess histological grade and response to therapy (*1*). As the article by Hiesiger et al. in the current issue of *The Journal of Nuclear Medicine* demonstrates, this laudable aim remains elusive: [^{11}C]putrescine, the high-profile PET brain-tumor tracer of the 1980s (*2,3*) has proved to be a disappointment in the 1990s. What lessons can be learned from the putrescine experience?

At first glance, the rationale for synthesizing ^{11}C-labeled putrescine seems unusually attractive. Endogenous putrescine, the immediate precursor of spermidine and spermine, is synthesized from ornithine by ornithine decarboxylase (ODC), the rate-limiting enzyme in polyamine synthesis (*4,5*). A second decarboxylase, S-adenosyl-L-methionine decarboxylase (SAMDC) catalyzes the formation of S-adenosyl-S-methylhomocysteamine, from which an aminopropyl moiety is transferred to putrescine to form spermidine, and to spermidine to form spermine (*4*). Whereas ODC activity and putrescine concentration are low in normal brain (*1,4,6*), elevated concentrations of di- and polyamines and their biosynthetic and catabolic enzymes have been reported in a wide variety of rapidly growing tissues, including primary and metastatic brain tumors (*4–8*). Finally, and perhaps most to the point, ODC activity, putrescine concentration and SAMDC activity in biopsy specimens of rat and human tumors, including gliomas, have been correlated with histopathological criteria of malignancy (*5,6,9–11*).

Although exogenously administered putrescine does not readily cross the intact blood-brain barrier (BBB), it rapidly traverses the more permeable blood-tumor barrier (*2,3,12*). Preliminary [^{14}C]putrescine autoradiographic studies in T9-gliosarcoma-bearing rats indicated that target-to-background (i.e., tumor-to-contralateral brain) concentration ratios as high as 35:1 were achievable and suggested that ^{11}C-labeled putrescine might serve as a "near ideal" PET tracer for the metabolic imaging of human brain tumors and, within the context of an appropriate pharmacodynamic model, as a marker for tumor growth rate (*2*). These high hopes were bolstered in 1987 by Hiesiger et al. (*3*), who reported in this journal that [^{11}C]putrescine PET studies of primary and metastatic brain tumors provided a better signal-to-noise ratio than glucose metabolic rate measurements obtained with [^{11}C]2-deoxyglucose (^{11}CDG); Hiesiger et al. also anticipated that [^{11}C]putrescine would prove useful for locating small glycolytically hypometabolic lesions and would provide a quantitative index of degree of malignancy.

But doubts began to emerge, even as new claims for [^{11}C]putrescine were being made. In their 1987 *Journal of Nuclear Medicine* article, Hiesiger et al. grappled with the possibility that some or all of the observed tumor uptake of plasma ^{11}C radioactivity ([^{11}C]putrescine, $^{11}CO_2$ and nonvolatile ^{11}C-labeled putrescine metabolites) was due to deficiency of the BBB, and that uptake of *exogenous* putrescine did not necessarily reflect the rate of tumor polyamine biosynthesis. In 1988, Warnick et al. reported surprisingly low in vivo rates of [exogenous] putrescine conversion to spermidine and spermine in T9 rat gliosarcoma

Received October 10, 1991; accepted October 10, 1991.

For reprints contact: D. A. Rottenberg, PET Imaging Service (11P), VA Medical Center, Minneapolis, Minnesota 55417.